

Inverse Problems and Imaging

Presentation - Project Assignment

Adonis JAMAL Jean-Vincent MARTINI
Reverse-time and Kirchhoff migration

Ecole Normale Supérieure Paris-Saclay
MVA 2025-2026

March 27th, 2026

école
normale
supérieure
paris-saclay



Overview and Objectives

Goal: Reconstruct the location of a point-like reflector from time-harmonic or broadband measurement data in 2D, using synthetic array data.

Configurations studied:

- **Full aperture:** circular array of N transducers
- **Partial aperture:** linear array along the x -axis
- **Time-dependent:** broadband signal emission
- **Noisy setting:** additive complex Gaussian noise

Methods compared:

Reverse-Time (RT) migration,
Kirchhoff Migration (KM),
MUSIC-type.

Workflow:

- ① Derive the Green's function and generate synthetic data via Born approximation
- ② Define and implement RT, KM, MUSIC functionals
- ③ Analyze results
- ④ Study stability under noise (Monte Carlo)

Green's Function and Data Model

Green's function. We assume propagation speed $c_0 = 1$. The 2D homogeneous Green's function $\hat{G}_0(\omega, x, y)$ satisfies:

$$\Delta_x \hat{G}_0 + \omega^2 \hat{G}_0 = -\delta(x - y), \quad x \in \mathbb{R}^2$$

with the Sommerfeld radiation condition. It is given explicitly by:

$$\hat{G}_0(\omega, x, y) = \frac{i}{4} H_0^{(1)}(\omega|x - y|)$$

where $H_0^{(1)}(s) = J_0(s) + iY_0(s)$ is the Hankel function of the first kind.

Data model (Born approximation). For a point-like reflector at \mathbf{x}_{ref} , the data matrix entry for receiver r and source s is:

$$\hat{u}_{rs}(\omega) = \omega^2 \hat{G}_0(\omega, \mathbf{x}_r, \mathbf{x}_{\text{ref}}) \hat{G}_0(\omega, \mathbf{x}_{\text{ref}}, \mathbf{x}_s)$$

which can be written in matrix form as:

$$\hat{U}(\omega) = -\frac{\omega^2}{16} \mathbf{v} \mathbf{v}^T, \quad v_t = H_0^{(1)}(\omega|\mathbf{x}_t - \mathbf{x}_{\text{ref}}|)$$

RT, KM and MUSIC Imaging Functionals

Reverse-Time (RT) migration:

$$\mathcal{I}_{RT}(\mathbf{x}) = \frac{1}{2\pi} \int_{-\infty}^{\infty} d\omega \sum_{r,s} \overline{\hat{G}_0(\omega, \mathbf{x}, \mathbf{x}_r)} \hat{u}_{rs}(\omega) \overline{\hat{G}_0(\omega, \mathbf{x}_s, \mathbf{x})}$$

Kirchhoff Migration (KM): from RT, with $\hat{G}_0(\omega, \mathbf{x}, \mathbf{y}) \approx e^{i\omega T(\mathbf{x}, \mathbf{y})}$:

$$\mathcal{I}_{KM}(\mathbf{x}) = \frac{1}{2\pi} \int_{-\infty}^{\infty} d\omega \sum_{r,s} e^{-i\omega|\mathbf{x}-\mathbf{x}_r|} \hat{u}_{rs}(\omega) e^{-i\omega|\mathbf{x}_s-\mathbf{x}|}$$

MUSIC (partial aperture, noise-subspace variant):

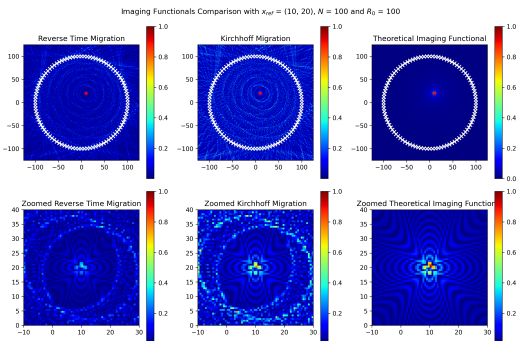
$$\mathcal{I}_{MU}(\mathbf{x}) = \frac{1}{1 - |\langle \hat{g}(\omega, \mathbf{x}), v_1 \rangle|^2}$$

where $\hat{g}(\omega, \mathbf{x}) = (\hat{G}_0(\omega, \mathbf{x}, \mathbf{x}_r))_{r=1,\dots,N}$ and v_1 is the first singular vector of \hat{U} .

Theoretical focal spots: Full aperture $\sim J_0^2(\omega|x - x_{ref}|)$; Partial aperture: sinc² in cross-range, Fresnel integral in range.

Full Aperture – RT, KM and Theoretical Focal Spot

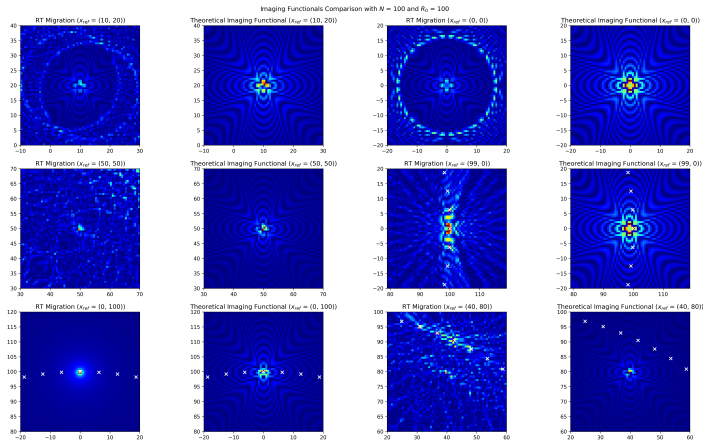
Setup: $N = 100$ transducers on a circle, $R_0 = 100$, $\omega = 2\pi$,
 $x_{\text{ref}} = (10, 20)$.



- RT and KM images are very similar; minor discrepancies come from the approximation used in KM.
- The theoretical J_0^2 focal spot differs noticeably: it is derived under the asymptotic limit $R_0 \rightarrow \infty$, $N \rightarrow \infty$.
- Near the reflector, all three profiles agree qualitatively.

Full Aperture – Multiple Reflector Positions

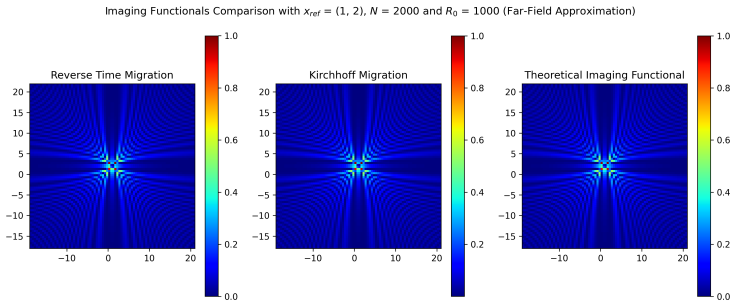
Effect of reflector position: reflector moved to $(0, 0)$, $(0, 100)$, $(100, 0)$.



As the reflector approaches the array boundary, the asymptotic assumptions break down and the discrepancy between RT/KM and the theoretical J_0^2 profile becomes more pronounced.

Full Aperture – Far-Field Regime

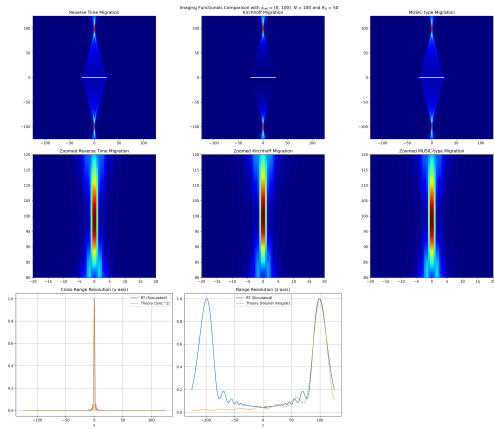
Far-field regime: $R_0 = 1000$, $N = 2000$.



With a much larger array and many more transducers, the RT and KM functionals converge closely to the theoretical J_0^2 focal spot, confirming the validity of the asymptotic formula in the appropriate regime.

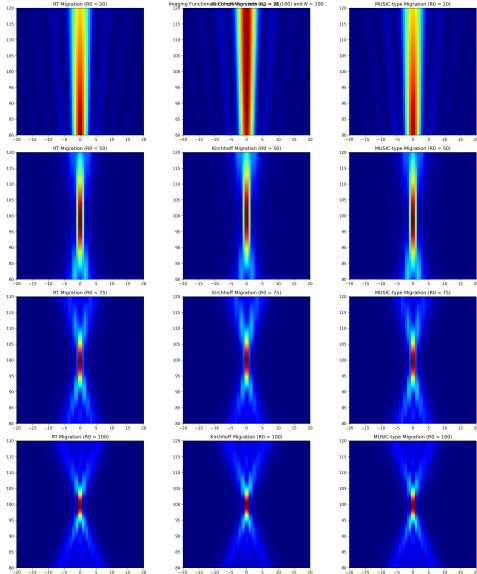
Partial Aperture – RT, KM and MUSIC

Setup: $N = 100$ transducers on a linear array, $R_0 = 100$, $\omega = 2\pi$, $\mathbf{x}_{\text{ref}} = (10, 20)$.



- RT, KM and MUSIC closely resemble each other.
- **Cross-range (x):** RT reproduces the main peak and secondary lobes; extra lobes arise from finite-aperture and discrete-sampling effects.
- **Range (z):** a mirror image appears at $-z_{\text{ref}}$ due to the linear geometry (transducers on the x -axis cannot distinguish z from $-z$).

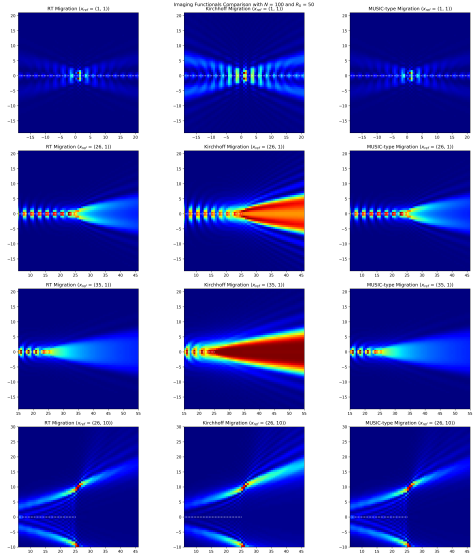
Partial Aperture – Influence of Array Length R_0



Varying R_0 : smaller aperture
⇒ coarser cross-range
resolution (larger
 $r_c = \lambda|x_{\text{ref}}|/R_0$).

As R_0 decreases, the focal spot widens in the cross-range direction, consistent with the theoretical sinc^2 prediction. The range resolution is unaffected by R_0 .

Partial Aperture – Multiple Reflector Positions

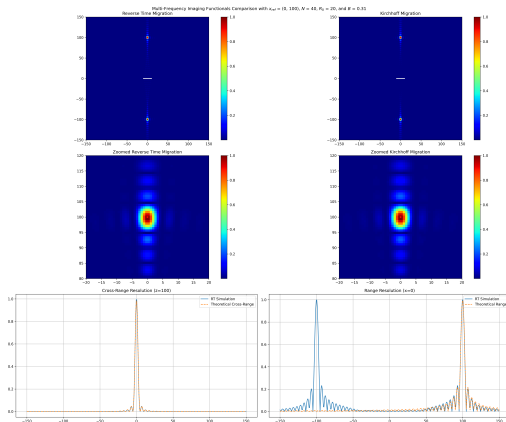


Varying x_{ref} : moving the reflector further from the array increases the range and degrades cross-range resolution.

The focal spot characteristics scale with the stand-off distance $|x_{\text{ref}}|$, in agreement with the theoretical expressions for r_c and r_f .

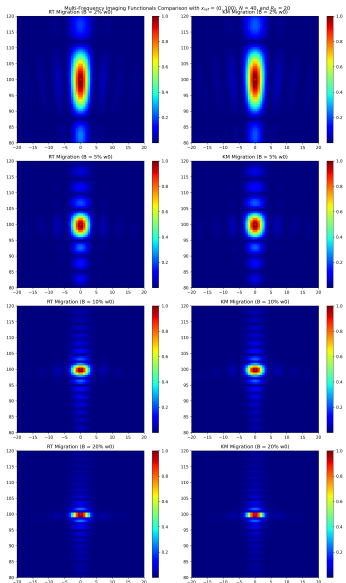
Time-Dependent (Broadband) – Partial Aperture

Setup: $N = 40$, $R_0 = 20$, broadband signal $\hat{f}(\omega) = \mathbf{1}_{[\omega_0-B, \omega_0+B]}(\omega)$, $\omega_0 = 2\pi$, $B = 0.05\omega_0$, $\mathbf{x}_{\text{ref}} = (0, 100)$.



- The focal spot is significantly more localized than in the monochromatic case: broader frequency content improves coherent focusing.
- Cross-range: RT matches the sinc^2 main peak (secondary lobes not captured due to discrete/finite array).
- Range: the profile is consistent with the theoretical $|\text{sinc}(2B|z - z_{\text{ref}}|)|$ prediction.

Time-Dependent – Influence of Bandwidth B



Varying bandwidth B : wider bandwidth \Rightarrow sharper range resolution ($r_I \propto 1/B$), cross-range resolution unchanged.

Increasing B dramatically reduces the range sidelobe level and sharpens the range profile, confirming the sinc dependence on bandwidth.

Stability – Noisy Model

Noise model. The recorded signals are perturbed by complex Gaussian noise:

$$\hat{u}_{rs}^{\text{noisy}}(\omega) = \hat{u}_{rs}(\omega) + W_{rs}^{(1)}(\omega) + i W_{rs}^{(2)}(\omega)$$

where $W_{rs}^{(1)}, W_{rs}^{(2)} \sim \mathcal{N}(0, \sigma^2/2)$ i.i.d.

Configurations revisited:

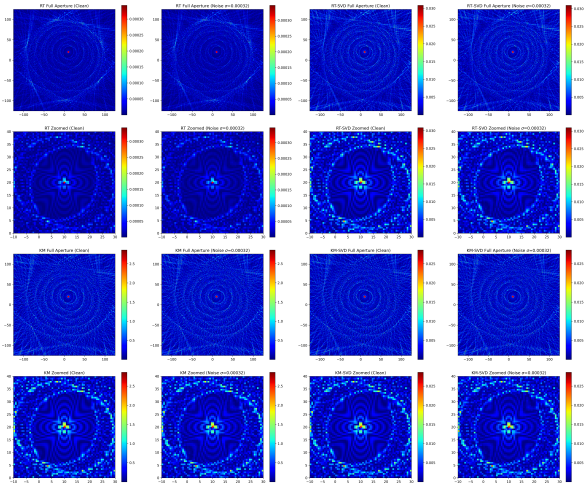
- Full aperture (RT & KM)
- Partial aperture (RT, KM & noise-subspace MUSIC)
- Time-dependent broadband (RT & KM)

Analysis: For each configuration, we plot images at increasing σ , then quantify localization error via Monte Carlo simulation (multiple noise realizations).

Note on MUSIC: we use the noise-subspace variant

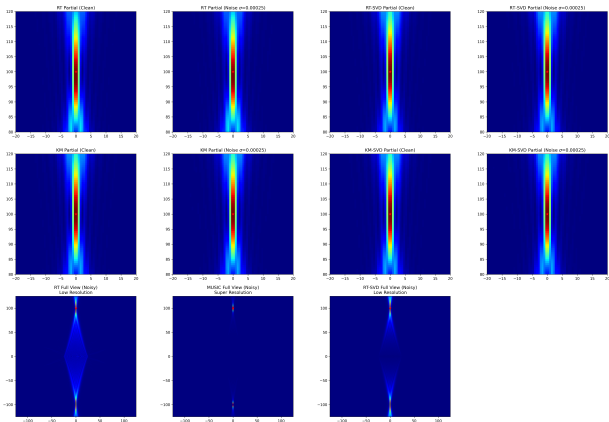
$\mathcal{I}_{MU}(\mathbf{x}) = 1/(1 - |\langle \hat{g}, v_1 \rangle|^2)$ to expose its super-resolution behaviour and its sensitivity to noise.

Stability – Full Aperture under Noise



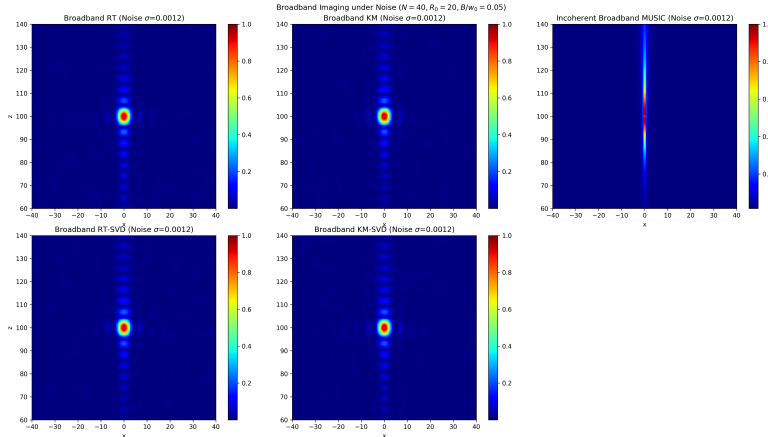
RT and KM both degrade gracefully as σ increases. Coherent integration over many transducer pairs provides a natural averaging effect that partially mitigates noise.

Stability – Partial Aperture under Noise



RT and KM remain robust for moderate noise levels. The noise-subspace MUSIC functional is sharper at low noise but degrades more abruptly: once the noise level is sufficient to perturb the dominant singular vector v_1 , the localization quality deteriorates rapidly.

Stability – Time-Dependent Broadband under Noise

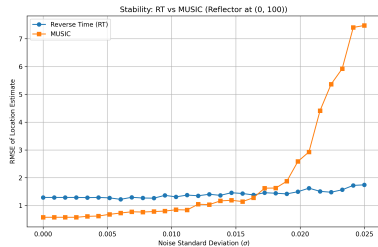


The broadband RT functional retains a well-defined peak even at elevated noise levels, benefiting from frequency diversity in addition to spatial averaging.

Stability – Monte Carlo Analysis: RT vs. MUSIC

RMSE of localization vs. noise level σ (multiple realizations, partial aperture).

- **RT:** localization error grows slowly and steadily with σ . Coherent back-propagation integrates over all source–receiver pairs, averaging out random noise contributions.
- **MUSIC:** error remains very low for small σ (super-resolution), then rises sharply beyond a threshold. Once noise corrupts the dominant singular vector v_1 , the functional fails abruptly.



⇒ RT is more robust; MUSIC offers higher precision at low noise but is fragile.

Conclusion

Summary of findings:

- **Full aperture:** RT and KM agree closely; both approach the theoretical J_0^2 focal spot as $R_0, N \rightarrow \infty$.
- **Partial aperture:** linear geometry introduces a mirror artifact in range; cross-range resolution scales as $r_c = \lambda|x_{\text{ref}}|/R_0$. MUSIC provides a sharper image.
- **Broadband:** increased bandwidth drastically improves range resolution ($r_l \propto 1/B$), consistent with sinc theory.
- **Noise:** RT migration degrades gracefully; MUSIC is precision-first but collapses beyond a noise threshold.

Perspectives:

- Extension to heterogeneous or anisotropic media.
- Advanced regularization to stabilize MUSIC at high noise.
- Investigation of multiple reflectors and mutual interference.
- Time-reversal approaches in random media.

Key take-away: Array geometry, bandwidth and noise level are the three dominant factors controlling resolution and stability of RT/KM imaging functionals.

Bibliography I

Ammari et al., *Mathematical and Statistical Methods for Multistatic Imaging*, Springer, 2013.